LEA: LEARNING LATENT EMBEDDING ALIGNMENT MODEL FOR fMRI DECODING AND ENCODING

Anonymous authors
Paper under double-blind review

ABSTRACT

The connection between brain activity and visual stimuli is crucial to understand the human brain. While deep generative models have exhibited advances in recovering brain recordings by generating images conditioned on fMRI signals, it is still challenge to generate consistent semantics. Moreover, the prediction of fMRI signal from visual stimuli remains a hard problem. In this paper, we introduce a unified framework that addresses both fMRI decoding and encoding. With training two latent spaces capable of representing and reconstructing fMRI signals and visual images, respectively, we align the fMRI signals and visual images within the latent space, thereby enabling a bidirectional transformation between the two domains. Our Latent Embedding Alignment (LEA) model concurrently recovers visual stimuli from fMRI signals and predicts brain activity from images within a unified framework under user-specified direction. The performance of LEA surpasses that of existing methods on multiple benchmark fMRI decoding and encoding datasets. LEA offers a comprehensive solution for modeling the relationship between fMRI signal and visual stimuli.

1 INTRODUCTION

The human brain exhibits dynamic responses to visual stimuli received through the eyes (Teng & Kravitz, 2019), and these responses can be indirectly measured using functional Magnetic Resonance Imaging (fMRI). Identifying and categorizing distinct patterns of brain activity in reaction to visual stimuli is a crucial step to understand the human brain. One approach to achieving this goal is through inverse modeling (Parthasarathy et al., 2017; Horikawa & Kamitani, 2017), which involves reconstructing the observed image from the fMRI signal. Since images contain a wealth of details that the brain may not fully capture, it is not necessary to reconstruct the visual stimuli with absolute precision. Consequently, researchers have primarily focused on decoding the semantic essence of images (Horikawa & Kamitani, 2017; Shen et al., 2019; Beliy et al., 2019; Gaziv et al., 2022). In contrast, fMRI encoding aims to predict the fMRI signal based on visual stimuli. It is worth noting that the semantic information contained in fMRI data is sparsely distributed and highly correlated between neighboring elements (Chang et al., 2019). As a result, the fMRI signal exhibits redundancy. Moreover, in practical scenarios, the available image-signal pairs is limited, posing a challenge to deploy deep learning methods that often rely on large training datasets for understanding fMRI data.

Recent researchs (Ozcelik et al., 2022; Ferrante et al., 2022; Chen et al., 2022; Liu et al., 2023; Du et al., 2023; Ozcelik & VanRullen, 2023) attempted to decode fMRI signals based on pre-trained generative models like Instance-Conditional GAN (Casanova et al., 2021), diffusion models (Ho et al., 2020), masked autoencoders (He et al., 2022), CLIP (Radford et al., 2021), to name a few. Despite achieving impressive results in high-fidelity generation, they face several challenges: (1) Despite their ability to generate images of exceptional quality, pre-trained generative models struggle to ensure semantic consistency with fMRI signals, presenting an ongoing challenge. (2) These models have demonstrated the capability to produce high-quality images even when provided with random noise disguised as fake fMRI signals (see Sec. 4 for details). This raises concerns about their reliability, particularly when dealing with a wide range of visual stimuli, including those not seen during training (open-vocabulary). This reliability issue is particularly relevant to fMRI decoding. Thus when utilizing large-scale pre-trained generative models for fMRI decoding, distinguishing

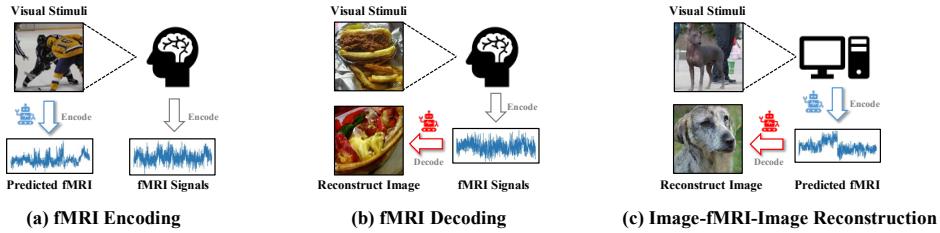

(a) fMRI Encoding (b) fMRI Decoding (c) Image-fMRI-Image Reconstruction

Figure 1: Our proposed LEA efficiently enables (a) fMRI encoding to estimate the brain activity from visual stimuli; (b) fMRI decoding to recover the visual stimuli from recorded fMRI signals, and (c) image-fMRI-image reconstruction to ensure the reliability of fMRI decoding and encoding.

between genuine fMRI signal decoding and unconditional image generation becomes a critical concern.

This paper, for the first time proposes a novel approach to address the challenges associated with fMRI signals by simultaneously tackling the tasks of fMRI decoding and encoding. Our method begins by side-stepping the necessity for paired image-fMRI data, instead opting for an encoder-decoder architecture designed specifically for fMRI signals and images. These encoder-decoder structures effectively learn dense and compact latent representation spaces, directly mitigating the issue of signal redundancy present in fMRI data. As a result, our model achieves the best performance on fMRI zero-shot classification where the categories of fMRI signals are unseen during training. Moreover, these encoder-decoder architectures can be trained via self-supervised learning techniques (Vincent et al., 2008; He et al., 2020; 2022), eliminating the need for additional supervision. Furthermore, this learned representation serves to reduce the feature dimensionality of both modalities, thus simplifying the task of transformation between them.

Technically, to align the two learned representation spaces effectively, we propose a lightweight alignment module that can be trained with a relatively small set of fMRI-image pairs. Alignment across diverse types of signals has been extensively explored in various vision-related tasks, such as image-text (Radford et al., 2021; Jia et al., 2021; Mahajan et al., 2018) and image-audio (Arandjelovic & Zisserman, 2017; Morgado et al., 2021; Owens & Efros, 2018; Patrick et al., 2020). These studies have revealed that well-encoded signals from different modalities can be effectively aligned within a shared representation space. However, given the absence of a large-scale fMRI-image paired dataset to support end-to-end training of such an alignment model, inspired by the linear relationships observed between text- and vision-only models (Merullo et al., 2023), we employ a linear regression model to learn the mapping between the two latent spaces. Empirical findings suggest that a similar linear relationship exists between fMRI- and vision-only models. Furthermore, this lightweight linear model can be trained with a small number of fMRI-image pairs, eliminating the need for a large-scale paired dataset and enabling the creation of individual-specific models. Within the framework of LEA, the alignment module serves a crucial role in assessing the reliability of both fMRI encoding and decoding models through the image-fMRI-image reconstruction assessment. By initially estimating fMRI signals from images and subsequently reconstructing the visual stimuli, the ability to generate semantically consistent images serves as a reliability indicator.

Consequently, we have devised the Latent Embedding Alignment (LEA) framework for fMRI decoding and encoding. LEA encompasses two distinct encoder-decoder architectures for handling fMRI signals and images, respectively. We introduce an alignment module to facilitate the transformation between the latent representation spaces of fMRI signals and images. As illustrated in Figure 1, when reconstructing visual stimuli from fMRI signals, we encode the fMRI signal, convert it into a latent image embedding, and subsequently decode it to generate images. Conversely, when predicting brain activities, we encode the images, transform them into latent fMRI embeddings, and then decode them to produce fMRI signals. An important feature of LEA is its support for image-fMRI-image reconstruction, which serves as a robust indicator of the reliability of both fMRI encoding and decoding models. Through extensive experiments on benchmark datasets, we demonstrate that LEA not only exhibits superiority in the domains of fMRI decoding and encoding.

Contribution. Our contributions can be succinctly summarized as follows:
1) **Encoder-Decoder Architectures**: We introduce specialized encoder-decoder architectures that learn latent representations for fMRI signals and images without the need for extensive paired training data. 2) **ROI-Induced Embedding Layer**: We devise an innovative ROI-induced embedding

layer to extract fMRI signals, ensuring geometric consistency in feature extraction. Additionally, we propose the use of global representations for fMRI signal reconstruction, promoting efficient feature compression. 3) **Latent Space Alignment**: We establish a linear connection between the latent spaces of fMRI and images, enabling seamless fMRI decoding and encoding within a unified framework called LEA. 4) **Superior Performance**: Through rigorous testing on multiple benchmark datasets, we demonstrate the exceptional performance of LEA, underscoring its effectiveness and significant advancements in the field of fMRI decoding and encoding.

2 Related Work

fMRI Coding encompasses both fMRI encoding and decoding. For fMRI encoding, it involves learning the mapping from visual stimuli to fMRI signals. Early studies (Yamins et al., 2013; 2014; Güçlü & van Gerven, 2015; Yamins & DiCarlo, 2016) primarily employed convolutional neural networks to extract semantic information from visual stimuli. However, with the resurgence of neural language models, recent research has successfully utilized models such as BERT (Devlin et al., 2018), Transformer (Vaswani et al., 2017), and GPT-2 (Radford et al., 2019) to predict fMRI responses from stimuli, including images and even words/sentences. Conversely, fMRI decoding focuses on the reverse mapping, from brain activity to stimuli. Previous studies (Mozafari et al., 2020; Ozcelik et al., 2022) developed regression models specifically designed to extract valuable information from fMRI signals. Ozcelik et al. (2022) employed a pre-trained Instance-Conditional GAN model (Casanova et al., 2021) to reconstruct images by decoding latent variables from fMRI data. Ferrante et al. (2022) utilized pre-trained latent diffusion models (Ho et al., 2020) to generate stimulus images by mapping fMRI signals to visual features. Beliy et al. (2019) adopted self-supervised learning on testing data to enable adaptation to testing statistics. Chen et al. (2022) introduced a self-supervised sparse masked modeling strategy to encode fMRI data into latent embeddings and fine-tuned latent diffusion models with double conditioning. In this paper, we present a unified framework that efficiently realizes both fMRI encoding and decoding.

Multi-Modality Alignment aims to establish connections across different modalities, such as image-text alignment (Radford et al., 2021; Jia et al., 2021; Mahajan et al., 2018) and image-audio alignment (Arandjelovic & Zisserman, 2017; Morgado et al., 2021; Owens & Efros, 2018; Patrick et al., 2020). Girdhar et al. (2023) endeavor to align multiple modalities within a unified latent representation space. The majority of efforts in this direction are centered around the CLIP model (Radford et al., 2021), which is trained on extensive image-text pairs to learn a shared latent space minimizing the distances between correlated image-text pairs. For instance, Liu et al. (2023) bridged the modality gap by leveraging CLIP's cross-modal generalization ability to address the limitation of limited fMRI-image paired data. Similarly, Du et al. (2023) employed multi-modal deep generative models to capture the relationships between brain, visual, and linguistic features. Ozcelik & VanRullen (2023) combined these techniques to predict multi-modal features from fMRI signals and generate reconstructed images using a latent diffusion model (Rombach et al., 2022).

3 Methodology

Problem Setup. Given fMRI signal $\mathbf{f}$ recorded from brain activity and the corresponding visual stimuli, image $\mathbf{I} \in \mathbb{R}^{H \times W \times 3}$, the purpose of our work is to learn a unified framework that can perform both **fMRI decoding** task that recovering the observed image from fMRI signal as well as **fMRI encoding** task that predicting the brain activity from the image.

For the decoding task, the ideal scenario involves the reconstructed images $\hat{\mathbf{I}}$ matching the real ones precisely. However, the unique nature of biological mechanisms suggests that individual memory or attention can influence an individual's brain activity response to the same image, and thus variations may occur. In light of this, we adhere to the approach introduced in (Mozafari et al., 2020; Ozcelik et al., 2022), requiring the recovered images $\hat{\mathbf{I}}$ to exhibit semantic consistency with $\mathbf{I}$. Consequently, our primary focus is on the **semantic fMRI decoding** task.

In the encoding task, it is challenging to make precise predictions of element-wise fMRI signals due to their inherent noise and redundancy. Therefore, in this paper, our focus shifts towards predicting the overall trends in fMRI signals. More specifically, we aim to generate estimated fMRI signals that exhibit a correlation with the actual fMRI signals. This correlation serves as an indicator of

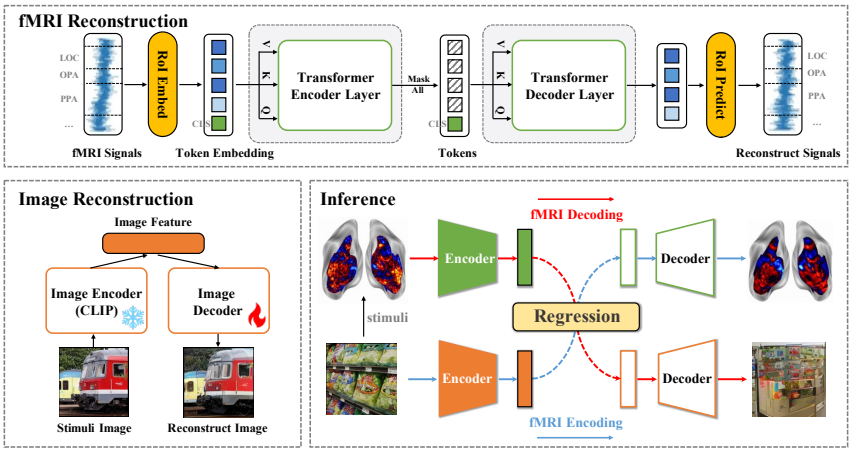

Figure 2: LEA Overview. We learn a latent representation space via the encoder-decoder architectures designed specifically for fMRI signals and images. Then a lightweight alignment module is proposed to link the two latent spaces, enabling joint fMRI encoding and decoding.

whether a Region-Of-Interest (ROI) region is activated or not. To achieve this goal, our objective is to produce estimated fMRI signals that maintain a linear relationship with the actual fMRI signals. This relationship can be assessed using Pearson correlation (Pearson's r).

3.1 Latent Space Construction for fMRI

The fMRI signals indirectly record neural activity in the visual cortex of the brain by measuring the blood-oxygen-level-dependent (BOLD) signals, which are usually represented as data of 3D voxels, covering visual regions, like early visual cortex (EVC), lateral occipital complex (LOC), occipital place area (OPA), parahippocampal place area (PPA), and retrosplenial complex (RSC) (Horikawa & Kamitani, 2015). Biological principles suggest that adjacent voxels in the brain's visual cortex often exhibit similar intensities in their stimulus-response (Ugurbil et al., 2013), resulting in redundancy within fMRI signals.

To investigate potential response patterns to visual stimuli and establish a reverse mapping for semantic encoding, it is essential to focus on the relationships among different regions while simultaneously capturing activity changes across long-range voxels. Inspired by the advantages of long-range receptive fields found in transformer layers, we follow Chen et al. (2022) by adopting masked autoencoder (He et al., 2022) as the encoder-decoder model for fMRI signals.

ROI embedding layer. Unlike Chen et al. (2022) that equally divides the fMRI signals into patches of equal size, we maintain the voxel structure with ROI regions. Specifically, we initially segment the fMRI signal vector (after standard pre-processing) into distinct ROI regions, each potentially having different dimensions. To address the dimension inconsistency, we propose the Region of Interest (ROI) Embedding layer. Given a specific ROI region i, denote the corresponding fMRI signal is of size $N_i \times 1$, indicating N_i voxels and 1 dimension of BOLD response, this fMRI signal region is first passed through a convolution layer with 32 kernels to extract multi-head features, resulting in dimensions of $N_i \times 32$. Subsequently, we employ a fully-connected layer to project the fMRI signal, which may have varying lengths, into a unified dimension of 1024. We then concatenate the embeddings from all ROI regions, yeilding the final input of size 32M$\times$1024, where M indicates the number of RoIs. Finally, we append a learnable [CLS] token to represent the "class" of the input.

Global feature extraction. In our encoder-decoder architecture training, we employ a masked auto-encoder (MAE) (He et al., 2022). The original MAE employs patch-based reconstruction, where a portion of the patches is masked, and the task is to predict these masked patches. While this approach is effective for learning local representations, it presents challenges when we aim to acquire a global latent code that represents the entire fMRI signal. To address this, we only preserve the global [CLS] token of the encoded fMRI singals, and mask all the patch-based latent code and let the decoder to learn to reconstruct fMRI signals from the learned [CLS] token. This strategy proves advantageous for learning a dense fMRI representation within the [CLS] token, and the trained decoder can subsequently used to generate fMRI signals based on the estimated latent fMRI code.

Finally, the decoder's output undergoes post-processing through a RoI Project layer. This layer mirrors the structure of the RoI Embed layer, effectively reversing the pre-processing applied to the fMRI signals, ensuring that the length matches that of the original fMRI signals. The overall model is trained by minimizing the L2 reconstruction loss of the fMRI signals.

$$\mathcal{L}_{fmri} = \frac{1}{M}\sum_{i=1}^{M} ||\mathbf{f}_i - \hat{\mathbf{f}}_i||_2^2, \tag{1}$$

where $\mathbf{f}_i$ and $\hat{\mathbf{f}}_i$ indicate the ground-truth and reconstructed fMRI signals, individually; M means the totally amount of training fMRI data.

3.2 Latent Space Construction for Image

The image-based latent space construction is a well-established domain of research. To recover semantic content from fMRI signals, we leverage pre-trained CLIP visual encoder as our foundation for image latent space. CLIP benefits from extensive training on large-scale image-text paired data, making its latent space rich in semantics and benefits the semantic consistency in our task.

Note that CLIP operates as an encoder-only model, and we cannot directly generate images from the image latent space. To address this issue, we adapt MaskGIT as our decoder to reconstruct images from the image latent space. In this approach, we fix the CLIP visual encoder and fine-tune the class-conditional MaskGIT as latent-conditional generative decoder. Further details regarding the objective functions can be found in (Chang et al., 2022).

3.3 Latent Embedding Alignment

Having established the fMRI and image latent spaces, the subsequent and pivotal step involves aligning these spaces to facilitate the simultaneous execution of fMRI decoding and encoding tasks. This approach diverges from previous methodologies (Du et al., 2023; Liu et al., 2023), which rely on additional modalities to bridge the gap between fMRI and image data. Instead, we advocate for the connection of well-represented latent features from both fMRI and image datasets using a linear model.

Furthermore, given the inherent instability of fMRI signals and the potential for distinct individual patterns within latent fMRI embeddings, we adopt an individual-specific approach. We train individual-specific linear models to establish mappings between personalized fMRI embeddings and image embeddings, and vice versa. We use L2 regularization, specifically through ridge regression, to constrain the learning space.

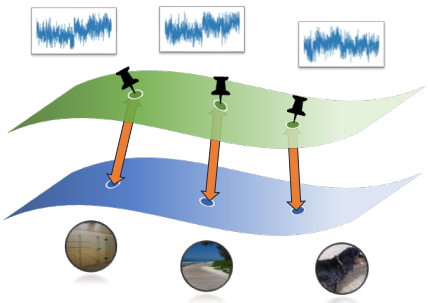

Figure 3: LEA aligns the latent space of fMRI signals and image features, enabling the bi-directional transformation.

With the construction of these two latent spaces and the acquisition of the latent embedding alignment module, we perform fMRI decoding and encoding tasks within a unified framework.

In the fMRI decoding task, we initially encode the fMRI signal within the learned latent fMRI space. Subsequently, we utilize the individual-specific linear model to project the latent fMRI code onto the latent visual feature space. This visual feature is then decoded using the fine-tuned class-conditional MaskGIT to recover the visual stimuli.

In the context of fMRI encoding, we first encode the CLIP visual feature and then project it onto the latent fMRI space through the individual-specific linear model. The projected latent fMRI code is subsequently decoded to estimate the actual fMRI signals.

4 Experiment

Datasets. We validate our LEA on Brain, Object, Landscape Dataset (BOLD5000) (Chang et al., 2019) and Generic Object Decoding Dataset (GOD) (Horikawa & Kamitani, 2017). (1) BOLD5000

Table 1: Top-1 accuracy of zero-shot classification on the GOD dataset.

METHOD	MODALITY	SBJ-1	SBJ-2	SBJ-3	SBJ-4	SBJ-5	AVERAGE
CADA-VAE (Schonfeld et al., 2019)	V&T	6.31	6.45	17.74	12.17	7.45	10.02
MVAE (Wu & Goodman, 2018)	V&T	5.77	5.40	17.11	14.02	7.89	10.04
MMVAE (Shi et al., 2019)	V&T	6.63	6.60	22.11	14.54	8.53	11.68
MoPoE-VAE (Sutter et al., 2021)	V&T	8.54	8.34	22.68	14.57	10.45	12.92
BrainCLIP-Linear (Liu et al., 2023)	V&T	10.00	12.00	18.00	12.00	12.00	12.80
CADA-VAE (Schonfeld et al., 2019)	V	5.66	6.01	16.51	9.17	6.01	8.67
MVAE (Wu & Goodman, 2018)	V	5.30	5.21	14.13	8.03	5.44	7.62
MMVAE (Shi et al., 2019)	V	5.41	5.39	13.76	10.62	5.02	8.04
MoPoE-VAE (Sutter et al., 2021)	V	5.20	7.42	14.05	9.25	6.37	8.46
BraVL (Du et al., 2023)	V	8.91	8.51	**18.17**	14.20	11.02	12.16
BrainCLIP (Liu et al., 2023)	V	6.00	16.00	16.00	14.00	**14.00**	13.20
LEA	V	**10.00**	**18.00**	12.00	**16.00**	12.00	**13.60**

Table 2: fMRI encoding comparison on Pearson's r metric (The higher the better).

METHOD	GOD						BOLD5000				
	Sbj-1	Sbj-2	Sbj-3	Sbj-4	Sbj-5	Avg.	CSI-1	CSI-2	CSI-3	CSI-4	Avg.
CLIP + MinD-Vis (Chen et al., 2022)	5.21	12.05	15.47	10.63	10.55	10.78	30.58	19.78	16.48	19.96	21.70
CLIP + Regressor (Gifford et al., 2023)	6.65	16.22	18.58	12.82	14.38	13.73	32.07	20.58	20.46	21.18	23.57
LEA($relax$)	8.43	15.51	**21.20**	**19.08**	15.07	15.86	34.32	**26.74**	27.74	**24.44**	28.19
LEA	**8.49**	**17.01**	20.58	17.82	**16.86**	**16.15**	**34.78**	25.91	**27.86**	24.37	**28.80**

encompasses a substantial fMRI-image dataset with a total of 5254 fMRI-image stimulus trials, involving four subjects. This dataset includes 1000, 2000, and 1916 images sourced from the Scene, COCO, and ImageNet datasets, respectively. Following the approach of Chen et al. (2022), we employ 4803 images from a single trial for training, reserving the remaining 113 images for testing. Our RoI Embed layer is configured with five pre-defined ROI regions (e.g., EV, LOC, OPA, PPA, RSC). (2) The GOD comprises data from 5 subjects, each viewing 1,250 images spanning 200 categories, resulting in a total of 1,250 fMRI-image pairs. We partition the training set into 1,200 pairs from 150 categories, while the remaining 50 categories are used exclusively for testing. The visual cortical ROI regions include V1, V2, V3, V4, FFA, PPA, LOC and HVC.

Metrics. For the fMRI decoding task, we utilize the following metrics for comprehensive comparisons: N-way Classification Accuracy (Acc) (Gaziv et al., 2022) to assess the semantic correctness of generated samples, Fréchet Inception Distance (FID) (Heusel et al., 2017) to evaluate the quality of generated images, and CLIP correlation and distance to gauge the semantic consistency of generated images. For Acc we calculate the average top-1 accuracy over 1,000 trials. For FID we use 64-dimensional features extracted by the Inception-v3 model to measure their similarity to ground-truth testing images. The CLIP distance represents the average CLIP similarity among all fMRI-image pairs, while CLIP correlation measures the correspondence of positive fMRI-image pairs compared to others. For the fMRI encoding task, we employ the Pearson's metric to assess the similarity between estimated fMRI signals and the ground-truth. We calculate the Pearson correlation on each vertex of the $N \times L$ matrix, where N represents fMRI signals from L vertices, and then average these correlations across different vertices.

Setting. We follow the general principle of not using any testing data in training. We denote our algorithm in this setting as LEA. Additionally, for a fair comparison with competitors, we follow the previous work (Chen et al., 2022; Beliy et al., 2019) and use the fMRI test set without revealing the label information. Specifically, the fMRI testing data is only trained for the reconstruction task via a self-supervised manner. When learning the latent embedding alignment module, we do not access any paired fMRI-image testing data, and the parameters of both fMRI and image reconstruction modules are frozen. These experiments are distinguished by adding the suffix of "relax" to the model name, as utilized in SSfMRI2IM (Beliy et al., 2019) and MinD-Vis (Chen et al., 2022).

Implementation. LEA is implemented using PyTorch. The fMRI reconstruction model is initialized with pre-trained weights from HCP datasets (Chen et al., 2022), but we randomly initialize parameters that do not match the dimensions of those from pre-trained weights (*e.g.*, RoI Embed layer). We further fine-tune it for each individual. The encoder and decoder have a depth of 24/8 with dimensions of 1024/512, and there are 16 multi-heads. For fine-tuning both models, we use the

Table 3: fMRI decoding performance comparison on the GOD dataset.

METRICS	METHODS	SBJ-1	SBJ-2	SBJ-3	SBJ-4	SBJ-5	AVERAGE
FID ↓	Gaziv et al. (2022)	7.67	2.67	2.51	8.93	2.77	4.91
	MinD-Vis (Chen et al., 2022)	1.97	1.63	1.68	1.77	2.33	1.88
	LEA(*relax*)	**1.45**	**1.43**	**1.52**	**1.48**	**1.25**	**1.23**
	LEA	2.57	1.51	1.67	1.71	1.34	1.76
CLIP Corr. ↑	Gaziv et al. (2022)	58.57	62.00	67.59	62.89	61.14	62.44
	MinD-Vis (Chen et al., 2022)	66.69	77.02	**83.78**	74.78	**80.04**	76.46
	LEA(*relax*)	**73.96**	78.20	80.94	**78.73**	70.86	76.54
	LEA	73.79	**79.63**	79.96	76.69	76.32	**77.28**
CLIP Dist. ↑	Gaziv et al. (2022)	0.31	0.34	0.34	0.32	0.32	0.33
	MinD-Vis (Chen et al., 2022)	0.33	0.35	**0.43**	0.38	0.39	0.38
	LEA(*relax*)	**0.38**	0.40	0.41	**0.40**	0.37	0.39
	LEA	**0.38**	**0.41**	0.40	0.39	**0.41**	**0.40**
Accuracy ↑	Gaziv et al. (2022)	1.88	3.79	12.99	8.45	6.26	6.67
	MinD-Vis (Chen et al., 2022)	9.10	15.91	**27.44**	15.81	14.28	16.51
	LEA(*relax*)	11.18	**18.62**	20.45	**20.04**	13.15	**16.69**
	LEA	**11.35**	18.55	18.92	17.52	**14.45**	16.16

Table 4: fMRI decoding performance comparison on BOLD5000 dataset.

METRICS	METHODS	CSI-1	CSI-2	CSI-3	CSI-4	AVERAGE
FID ↓	MinD-Vis (Chen et al., 2022)	**1.20**	1.90	**1.40**	1.32	1.46
	Ours	1.31	**1.53**	1.48	**1.19**	**1.38**
CLIP Corr. ↑	MinD-Vis (Chen et al., 2022)	**88.29**	-	-	83.09	-
	Ours	86.60	83.56	83.82	**84.77**	84.69
CLIP Dist. ↑	MinD-Vis (Chen et al., 2022)	0.41	-	-	0.37	-
	Ours	**0.41**	0.38	0.37	**0.39**	0.39
Accuracy ↑	MinD-Vis (Chen et al., 2022)	**29.94**	18.50	**21.00**	20.37	22.45
	Ours	28.48	**19.74**	19.65	**22.48**	**22.59**

AdamW optimizer with hyperparameters $\beta_1 = 0.9$, $\beta_1 = 0.95$, and a batch size of 8. The initial learning rate is set to 5e-5 with a weight decay of 0.01. We apply a linear learning rate schedule, gradually reducing the learning rate until it reaches the minimum value. The total number of training iterations for the fMRI reconstruction model is 100k, and for image reconstruction model, it is 300k.

4.1 MAIN RESULTS

Analysis of zero-shot classification. As we inherit the latent space from the original CLIP model, LEA enables open-vocabulary recognition of fMRI signals. To assess this capability, we perform experiments on zero-shot fMRI signal classification tasks to identify the most similar category for each fMRI signal. Specifically, we create a set of candidate class names using various text templates. These class names are then encoded using the CLIP text encoder. Subsequently, we calculate the similarity between the class embeddings and the fMRI latent embeddings learned by LEA.

We conduct experiments on the GOD, which contains 50 visual stimuli from 50 categories that are unseen during training. We report the top-1 classification accuracy (with the chance levels of 2%) of several competitors in Table 1. Results of competitors are from Liu et al. (2023). We divide the competitors into two groups based on their supervision modality, where V indicates visual supervision only and V&T indicates bothe visual and textual supervision. Our LEA trained with visual supervision beats all competitors, indicating the superiority of our bi-directional transformation.

Analysis of fMRI encoding. With two latent spaces for fMRI signal and image, LEA can not only recover the visual stimuli but also predict fMRI signal by visual image. As in Table 2, we conduct experiments to validate the estimation capability of our LEA. We construct two competitors to show the effectiveness of LEA. The 'CLIP+Regressor' means that we apply liner regression to directly generate fMRI signal based over the image feature from CLIP model. With the absent of learned fMRI embedding in LEA, the 'CLIP+Regressor' adopts the pipeline of 'image features → fMRI signals' instead of 'image features → fMRI features → fMRI signals'. However, such method causes misalignment of features during reconstruction without the fMRI latent space, as validated in

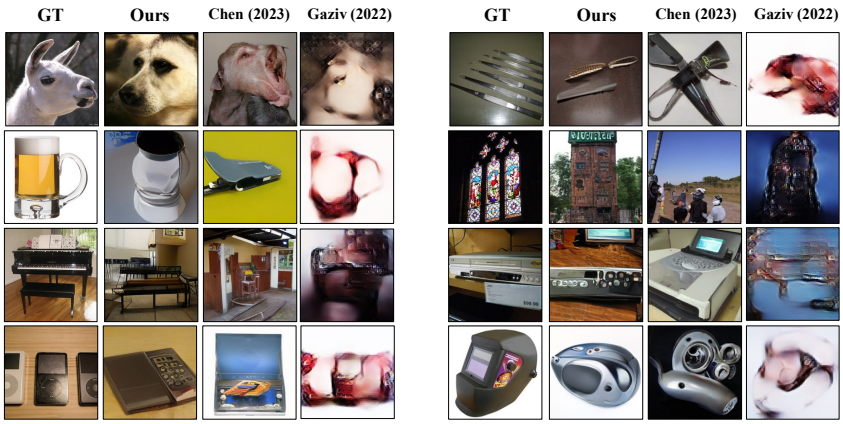

Figure 4: fMRI decoding performance comparison on the GOD dataset.

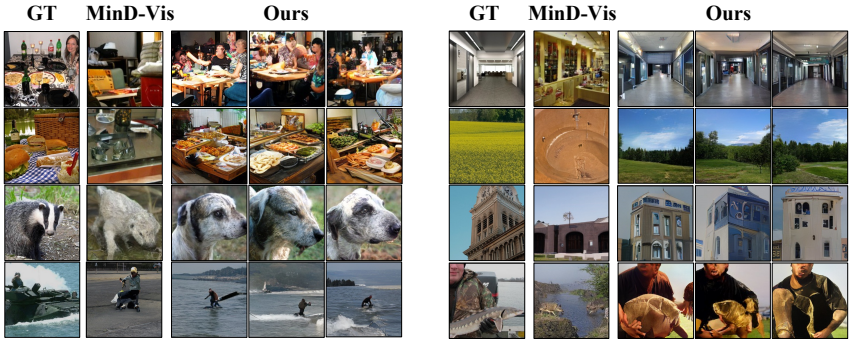

Figure 5: fMRI decoding performance comparison on BOLD5000 dataset.

the empirical results. The 'CLIP+MinD-Vis' utilizes the transformer decoder to predict fMRI signal from image CLIP feature. Such solution is too rough and not conducive to fine-grained feature alignment and generation. Our LEA achieves the best Pearson's score, which indicates that the alignment between latent embedding spaces are more effective for fMRI prediction.

Analysis of fMRI decoding. We present a comprehensive comparison of fMRI decoding performance on the GOD and BOLD5000 datasets in Table 3 and Table 4, respectively. To ensure a fair assessment, we reproduce the results of competitors using their official released models. It is worth noting that due to the availability of the official model of CIS-1,4 on the BOLD5000 dataset in MinD-Vis, we exclusively report the reproduced CLIP scores for these two individuals. Our novel LEA consistently demonstrates superior performance across various perspectives, including image quality, semantic correctness, and correlation, on both the GOD and BOLD5000 datasets. Notably, LEA excels in generating images of higher quality than its competitors on the GOD dataset. While MinD-Vis may outperform LEA on specific subjects, it significantly lags behind LEA on others, such as SUB-1,2,4 in the GOD and CSI-2,4 in BOLD5000, resulting in an overall inferior average performance. In summary, LEA not only outperforms current competitors in fMRI decoding but also possesses the capability for fMRI encoding, making it a comprehensive and superior solution in the field.

4.2 Qualitative Results and Further Analysis

To intuitively illustrate the efficacy of our method, we show some generated images in Figure 4 and Figure 5 for the GOD and BOLD5000 datasets, respectively. We compare with MinD-Vis (Chen et al., 2022) and Gaziv et al. (2022) on the GOD and MinD-Vis on BOLD5000.

Qualitative results. Our generated images consistently maintain the same semantic information as the ground-truth, encompassing humans, objects, animals, architecture, and landscapes. In contrast, competitors may falter in some instances, failing to preserve semantic consistency. For instance, in

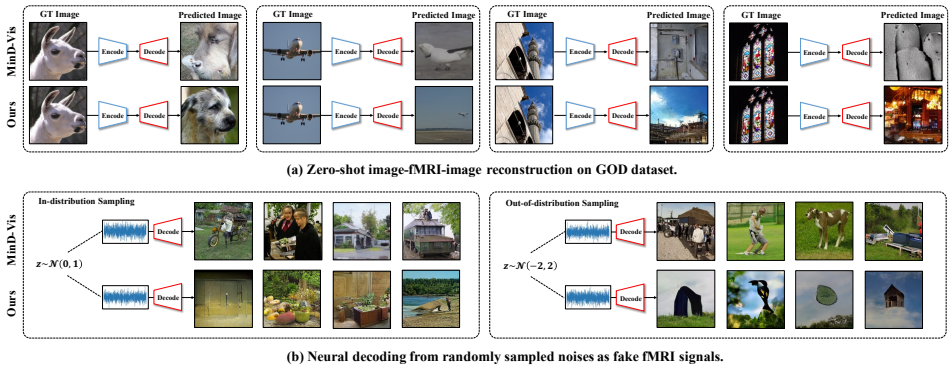

(a) Zero-shot image-fMRI-image reconstruction on GOD dataset.

(b) Neural decoding from randomly sampled noises as fake fMRI signals.

Figure 6: Reliable fMRI decoding analysis.

Figure 4, LEA excels in producing semantic-consistent and high-fidelity images, whereas competitors struggle to preserve semantics. In the last row on the left side of Figure 5, MinD-Vis can only generate a person while neglecting the water, whereas LEA consistently generates both the person and the water. These results highlight our ability to not only maintain the correctness of objects but also capture finer-grained semantics. Moreover, our approach achieves image fidelity in numerous cases, contributing to a more comprehensive and effective solution.

Reliable fMRI decoding. Ensuring the accuracy of fMRI decoding models is paramount, as they should decode brain activities rather than merely generate images without meaningful context. However, current approaches often rely on large pre-trained generative models capable of high-fidelity image generation, even when conditioned on random noise. This raises concerns about whether such high-quality images truly reflect brain activities, especially in zero-shot scenarios where the fMRI signals were not part of the training data. To assess the reliability of fMRI decoding models, we conduct two experiments:

(1) **Zero-shot image-fMRI-image reconstruction**: In this task, we use a novel image to estimate the fMRI signals, then use the estimated fMRI signals to reconstruct the image. Successful image-fMRI-image reconstruction implies better semantic consistency for encoding and decoding.

(2) **fMRI-image with random noise as fake fMRI signals**: In this task, we randomly generate fMRI signals from a Gaussian distribution, which significantly deviates from the real fMRI signal distribution. We then decode these fake fMRI signals to generate images. The reconstructed image should contain non-semantic information, indicating non-informative fMRI signals.

It is important to note that these tasks are not intended to demonstrate the superiority of a model on new tasks but rather to assess the reliability of methods designed for visual decoding. As shown in Figure 6, LEA excels in the image-fMRI-image reconstruction task while generating unrealistic and non-informative images when conditioned on fake fMRI signals that deviate from the distribution of real fMRI signals. In contrast, MinD-Vis performs poorly on the image-fMRI-image reconstruction task, generating high-fidelity and informative images when conditioned on random noise. These findings underscore that existing models have not thoroughly explored the reliability of fMRI decoding models. In comparison, both the fMRI decoding and encoding components of LEA demonstrate greater reliability than current algorithms.

5 Conclusions

In this paper, we address the challenge of jointly performing fMRI decoding and encoding within a single, unified framework. Our proposed Latent Embedding Alignment (LEA) not only constructs latent spaces for fMRI signals and images but also aligns them, enabling bidirectional transformation. By mitigating issues related to redundancy, instability, and data scarcity in fMRI datasets, LEA excels at producing high-fidelity, semantically consistent fMRI decoding results. Moreover, LEA demonstrates the capability to accurately estimate human brain activity from visual stimuli through fMRI encoding. Our experimental results on two benchmark datasets validate the effectiveness of LEA, highlighting its significant contributions in the field.

REFERENCES

Relja Arandjelovic and Andrew Zisserman. Look, listen and learn. In *Proceedings of the IEEE international conference on computer vision*, pp. 609–617, 2017.

Roman Beliy, Guy Gaziv, Assaf Hoogi, Francesca Strappini, Tal Golan, and Michal Irani. From voxels to pixels and back: Self-supervision in natural-image reconstruction from fmri. *Advances in Neural Information Processing Systems*, 32, 2019.

Arantxa Casanova, Marlene Careil, Jakob Verbeek, Michal Drozdzal, and Adriana Romero Soriano. Instance-conditioned gan. *Advances in Neural Information Processing Systems*, 34:27517–27529, 2021.

Huiwen Chang, Han Zhang, Lu Jiang, Ce Liu, and William T. Freeman. Maskgit: Masked generative image transformer. In *IEEE/CVF Conference on Computer Vision and Pattern Recognition, CVPR 2022, New Orleans, LA, USA, June 18-24, 2022*, pp. 11305–11315. IEEE, 2022.

Nadine Chang, John A Pyles, Austin Marcus, Abhinav Gupta, Michael J Tarr, and Elissa M Aminoff. Bold5000, a public fmri dataset while viewing 5000 visual images. *Scientific data*, 6(1):49, 2019.

Zijiao Chen, Jiaxin Qing, Tiange Xiang, Wan Lin Yue, and Juan Helen Zhou. Seeing beyond the brain: Conditional diffusion model with sparse masked modeling for vision decoding. *arXiv preprint arXiv:2211.06956*, 2022.

Jia Deng, Wei Dong, Richard Socher, Li-Jia Li, Kai Li, and Li Fei-Fei. Imagenet: A large-scale hierarchical image database. In *2009 IEEE conference on computer vision and pattern recognition*, pp. 248–255. Ieee, 2009.

Jacob Devlin, Ming-Wei Chang, Kenton Lee, and Kristina Toutanova. Bert: Pre-training of deep bidirectional transformers for language understanding. *arXiv preprint arXiv:1810.04805*, 2018.

Changde Du, Kaicheng Fu, Jinpeng Li, and Huiguang He. Decoding visual neural representations by multimodal learning of brain-visual-linguistic features. *IEEE Transactions on Pattern Analysis and Machine Intelligence*, 2023.

Matteo Ferrante, Tommaso Boccato, and Nicola Toschi. Semantic brain decoding: from fmri to conceptually similar image reconstruction of visual stimuli. *CoRR*, abs/2212.06726, 2022.

Guy Gaziv, Roman Beliy, Niv Granot, Assaf Hoogi, Francesca Strappini, Tal Golan, and Michal Irani. Self-supervised natural image reconstruction and large-scale semantic classification from brain activity. *NeuroImage*, 254:119121, 2022.

Alessandro T Gifford, Benjamin Lahner, Sari Saba-Sadiya, Martina G Vilas, Alex Lascelles, Aude Oliva, Kendrick Kay, Gemma Roig, and Radoslaw M Cichy. The algonauts project 2023 challenge: How the human brain makes sense of natural scenes. *arXiv preprint arXiv:2301.03198*, 2023.

Rohit Girdhar, Alaaeldin El-Nouby, Zhuang Liu, Mannat Singh, Kalyan Vasudev Alwala, Armand Joulin, and Ishan Misra. Imagebind: One embedding space to bind them all. *arXiv preprint arXiv:2305.05665*, 2023.

Umut Güçlü and Marcel AJ van Gerven. Deep neural networks reveal a gradient in the complexity of neural representations across the ventral stream. *Journal of Neuroscience*, 35(27):10005–10014, 2015.

Kaiming He, Haoqi Fan, Yuxin Wu, Saining Xie, and Ross Girshick. Momentum contrast for unsupervised visual representation learning. In *Proceedings of the IEEE/CVF conference on computer vision and pattern recognition*, pp. 9729–9738, 2020.

Kaiming He, Xinlei Chen, Saining Xie, Yanghao Li, Piotr Dollár, and Ross Girshick. Masked autoencoders are scalable vision learners. In *Proceedings of the IEEE/CVF Conference on Computer Vision and Pattern Recognition*, pp. 16000–16009, 2022.

Martin Heusel, Hubert Ramsauer, Thomas Unterthiner, Bernhard Nessler, and Sepp Hochreiter. Gans trained by a two time-scale update rule converge to a local nash equilibrium. *Advances in neural information processing systems*, 30, 2017.

Jonathan Ho, Ajay Jain, and Pieter Abbeel. Denoising diffusion probabilistic models. *Advances in Neural Information Processing Systems*, 33:6840–6851, 2020.

Tomoyasu Horikawa and Yukiyasu Kamitani. Generic decoding of seen and imagined objects using hierarchical visual features. *CoRR*, abs/1510.06479, 2015.

Tomoyasu Horikawa and Yukiyasu Kamitani. Generic decoding of seen and imagined objects using hierarchical visual features. *Nature communications*, 8(1):15037, 2017.

Chao Jia, Yinfei Yang, Ye Xia, Yi-Ting Chen, Zarana Parekh, Hieu Pham, Quoc Le, Yun-Hsuan Sung, Zhen Li, and Tom Duerig. Scaling up visual and vision-language representation learning with noisy text supervision. In *International Conference on Machine Learning*, pp. 4904–4916. PMLR, 2021.

Yulong Liu, Yongqiang Ma, Wei Zhou, Guibo Zhu, and Nanning Zheng. Brainclip: Bridging brain and visual-linguistic representation via clip for generic natural visual stimulus decoding from fmri. *arXiv preprint arXiv:2302.12971*, 2023.

Dhruv Mahajan, Ross Girshick, Vignesh Ramanathan, Kaiming He, Manohar Paluri, Yixuan Li, Ashwin Bharambe, and Laurens Van Der Maaten. Exploring the limits of weakly supervised pretraining. In *Proceedings of the European conference on computer vision (ECCV)*, pp. 181–196, 2018.

Jack Merullo, Louis Castricato, Carsten Eickhoff, and Ellie Pavlick. Linearly mapping from image to text space. In *The Eleventh International Conference on Learning Representations*, 2023. URL https://openreview.net/forum?id=8tYRqb05pVn.

Pedro Morgado, Nuno Vasconcelos, and Ishan Misra. Audio-visual instance discrimination with cross-modal agreement. In *Proceedings of the IEEE/CVF Conference on Computer Vision and Pattern Recognition*, pp. 12475–12486, 2021.

Milad Mozafari, Leila Reddy, and Rufin VanRullen. Reconstructing natural scenes from fmri patterns using bigbigan. In *2020 International Joint Conference on Neural Networks, IJCNN 2020, Glasgow, United Kingdom, July 19-24, 2020*, pp. 1–8. IEEE, 2020.

Andrew Owens and Alexei A Efros. Audio-visual scene analysis with self-supervised multisensory features. In *Proceedings of the European Conference on Computer Vision (ECCV)*, pp. 631–648, 2018.

Furkan Ozcelik and Rufin VanRullen. Brain-diffuser: Natural scene reconstruction from fmri signals using generative latent diffusion. *arXiv preprint arXiv:2303.05334*, 2023.

Furkan Ozcelik, Bhavin Choksi, Milad Mozafari, Leila Reddy, and Rufin VanRullen. Reconstruction of perceived images from fmri patterns and semantic brain exploration using instance-conditioned gans. In *International Joint Conference on Neural Networks, IJCNN 2022, Padua, Italy, July 18-23, 2022*, pp. 1–8. IEEE, 2022.

Nikhil Parthasarathy, Eleanor Batty, William Falcon, Thomas Rutten, Mohit Rajpal, EJ Chichilnisky, and Liam Paninski. Neural networks for efficient bayesian decoding of natural images from retinal neurons. *Advances in Neural Information Processing Systems*, 30, 2017.

Mandela Patrick, Yuki Asano, Polina Kuznetsova, Ruth Fong, Joao F Henriques, Geoffrey Zweig, and Andrea Vedaldi. Multi-modal self-supervision from generalized data transformations. *openreview.net*, 2020.

Alec Radford, Jeffrey Wu, Rewon Child, David Luan, Dario Amodei, Ilya Sutskever, et al. Language models are unsupervised multitask learners. *OpenAI blog*, 1(8):9, 2019.

Alec Radford, Jong Wook Kim, Chris Hallacy, Aditya Ramesh, Gabriel Goh, Sandhini Agarwal, Girish Sastry, Amanda Askell, Pamela Mishkin, Jack Clark, et al. Learning transferable visual models from natural language supervision. In *International conference on machine learning*, pp. 8748–8763. PMLR, 2021.

Robin Rombach, Andreas Blattmann, Dominik Lorenz, Patrick Esser, and Björn Ommer. High-resolution image synthesis with latent diffusion models. In *Proceedings of the IEEE/CVF Conference on Computer Vision and Pattern Recognition*, pp. 10684–10695, 2022.

Edgar Schonfeld, Sayna Ebrahimi, Samarth Sinha, Trevor Darrell, and Zeynep Akata. Generalized zero-and few-shot learning via aligned variational autoencoders. In *Proceedings of the IEEE/CVF Conference on Computer Vision and Pattern Recognition*, pp. 8247–8255, 2019.

Guohua Shen, Kshitij Dwivedi, Kei Majima, Tomoyasu Horikawa, and Yukiyasu Kamitani. End-to-end deep image reconstruction from human brain activity. *Frontiers in computational neuroscience*, 13:21, 2019.

Yuge Shi, Brooks Paige, Philip Torr, et al. Variational mixture-of-experts autoencoders for multi-modal deep generative models. *Advances in Neural Information Processing Systems*, 32, 2019.

Thomas M Sutter, Imant Daunhawer, and Julia E Vogt. Generalized multimodal elbo. *arXiv preprint arXiv:2105.02470*, 2021.

Chunyue Teng and Dwight J Kravitz. Visual working memory directly alters perception. *Nature human behaviour*, 3(8):827–836, 2019.

Kâmil Ugurbil, Junqian Xu, Edward J. Auerbach, Steen Moeller, An T. Vu, Julio Martin Duarte-Carvajalino, Christophe Lenglet, Xiaoping Wu, Sebastian Schmitter, Pierre-François van de Moortele, John P. Strupp, Guillermo Sapiro, Federico De Martino, Dingxin Wang, Noam Harel, Michael Garwood, Liyong Chen, David A. Feinberg, Stephen M. Smith, Karla L. Miller, Stamatios N. Sotiropoulos, Saâd Jbabdi, Jesper L. R. Andersson, Timothy Edward John Behrens, Matthew F. Glasser, David C. Van Essen, and Essa Yacoub. Pushing spatial and temporal resolution for functional and diffusion MRI in the human connectome project. *NeuroImage*, 80:80–104, 2013.

Ashish Vaswani, Noam Shazeer, Niki Parmar, Jakob Uszkoreit, Llion Jones, Aidan N. Gomez, Lukasz Kaiser, and Illia Polosukhin. Attention is all you need. In Isabelle Guyon, Ulrike von Luxburg, Samy Bengio, Hanna M. Wallach, Rob Fergus, S. V. N. Vishwanathan, and Roman Garnett (eds.), *Advances in Neural Information Processing Systems 30: Annual Conference on Neural Information Processing Systems 2017, December 4-9, 2017, Long Beach, CA, USA*, pp. 5998–6008, 2017.

Pascal Vincent, Hugo Larochelle, Yoshua Bengio, and Pierre-Antoine Manzagol. Extracting and composing robust features with denoising autoencoders. In *Proceedings of the 25th international conference on Machine learning*, pp. 1096–1103, 2008.

Mike Wu and Noah Goodman. Multimodal generative models for scalable weakly-supervised learning. *Advances in neural information processing systems*, 31, 2018.

Daniel L Yamins, Ha Hong, Charles Cadieu, and James J DiCarlo. Hierarchical modular optimization of convolutional networks achieves representations similar to macaque it and human ventral stream. *Advances in neural information processing systems*, 26, 2013.

Daniel LK Yamins and James J DiCarlo. Using goal-driven deep learning models to understand sensory cortex. *Nature neuroscience*, 19(3):356–365, 2016.

Daniel LK Yamins, Ha Hong, Charles F Cadieu, Ethan A Solomon, Darren Seibert, and James J DiCarlo. Performance-optimized hierarchical models predict neural responses in higher visual cortex. *Proceedings of the national academy of sciences*, 111(23):8619–8624, 2014.

SUPPLEMENTARY MATERIALS

The supplementary document is organized as follows:

- Sec. A introduces implementation details, including data augmentation, training and testing procedures.
- Sec. B provides ablation studies to investigate the effectiveness of our proposed RoI-dependent processing layer.
- Sec. C visualize more qualitative results of fMRI decoding and image-fMRI-image reconstruction, further showing the efficacy and advancements of our model.
- Sec. D discusses the broader impact of our work.

A. IMPLEMENTATION DETAILS

A.1. MODEL ARCHITECTURES

Our proposed Latent Embedding Alignment (LEA) framework aims to build the bridge between images and fMRI signals. To this end, we incorporates two distinct encoder-decoder architectures to learn latent representations for these two modalities by performing the self-supervised reconstruction task. Subsequently, we introduce a linear model to efficiently facilitate the transformation between the latent representation spaces of images and fMRI signals.

fMRI Reconstruction. We adopt the architecture of masked autoencoder (He et al., 2022) as the encoder-decnoder model for fMRI signals. More concretely, the fMRI encoder consists of 24 transformer layers, each of which has 1024 feature dimensions with 16 heads. We append a [CLS] token to the input fMRI signals before feeding them into the fMRI encoder. After self-attention processing, the [CLS] token is expected to capture the global representation of the entire input fMRI signals. Next, we mask all other latent token, and encourage the decoder to reconstruct fMRI signals from the learned [CLS] token. Similarly, the decoder includes 8 transformer layers, with 512 feature dimensions and 16 heads. Different from (Chen et al., 2022) that equally splits fMRI signals into patches, we instead maintain the voxel structure with RoI regions by additionally adding RoI-dependent processing layers (*i.e.*, RoI Embed and RoI Predict) before and after the encoder and decoder, respectively. Both RoI-dependent layers are two-layer modules with the symmetric structure and not shared among different RoI regions. Taking RoI Embed layer as an example, it first adopts a convolution layer with 32 kernels to extract multi-head features of input fMRI signal, and then uses a fully-connected layer to project the different length of fMRI signal into a unified dimension of 1024, leading to the final fMRI embeddings for one RoI as 32×1024.

Image Reconstruction. Image-based latent space construction has been widely investigated. As our target is to recoder the semantic content of fMRI signals, we adopt the pre-trained CLIP (ViT-H/14)[1] as the image encoder and the yielding CLIP latent space as our image latent space. To generate images from the image latent space, we utilize MaskGIT[2] as the image decoder in this paper, but other generative models are also acceptable. Specifically, the decoder is a decoder-only transformer layer, with the depth of 24, the feature dimension of 768 and 16 heads. By conditioned on the image latent features, the generation procedure starts from all [MASK] tokens and autoregressively predicts logits of tokens with higher confident scores. It is a non-sequential generative procedure, following a cosine mask scheduling function.

A.2. DATA AUGMENTATION

We utilize data augmentation to enlarge training data for both fMRI and image reconstruction, and discard them all during the inference or the fitting of linear models. For fMRI signals, we only use one augmentation method by randomly adding Gaussian noise with the probability of 0.25. For image data, we apply random cropping, random horizontal flipping and finally resize images to 256×256.

[1] https://github.com/mlfoundations/open_clip
[2] https://github.com/google-research/maskgit

Table 5: Classification Accuracy of CSI-1 on BOLD5000 dataset

METHODS	8	16	24	32	64	96
PatchEmbed	-	26.38	-	-	-	-
RoIEmbed	24.75	24.35	26.69	**28.48**	23.96	26.08

A.3. TRAINING AND TESTING PROCEDURES

All experiments are implemented with the PyTorch toolkit. The encoder-decoder model for fMRI reconstruction is initialized with pre-trained weights from HCP datasets (Chen et al., 2022). We finetune it with both fMRI training and testing sets for each individual. Note that using fMRI testing data is a common practice as in (Chen et al., 2022; Beliy et al., 2019), and we do not access any paired fMRI-image testing data when learning linear models. For image reconstruction, we use frozen CLIP encoder and utilize the image decoder of MaskGIT initialized by ImageNet (Deng et al., 2009), and further finetune it with images from the training sets on both the GOD and BOLD5000 datasets. Once trained, it is shared for all subjects and experiments. AdamW optimizer is applied with $\beta_1 = 0.9$, $\beta_1 = 0.95$ and batch size 8 to finetune both models. The initial learning rate is defined as 5e-5 with 0.01 weight decay. We linear decrease the learning rate until it reaches to the minimal rate. The total number of training iterations for fMRI reconstruction and image reconstruction is 100k and 300k. For fitting linear models, we adopt ridge regression from Scipy library. The coefficient of L2 regularization term α is set to 500 for both image-to-fMRI and fMRI-to-image regressions. During the inference of fMRI decoding, the number of steps for MaskGIT is 11 as default, and we generate 5 samples for all evaluations.

B. FURTHER ANALYSIS

Without loss of generality, experiments in this section are conducted on CSI-1 of BOLD5000 dataset.

B.1. EFFECTIVENESS OF THE ROI-DEPENDENT PROCESSING LAYER

Human brains are known to spatially separated, that different RoI regions react to different visual stimulus. Preserving the spatial structure is beneficial to help understanding the fMRI signals. Therefore, we design RoI Embed layers ('RoIEmbed' for short) to separately encode signals from different RoI regions. Differently, previous methods (Chen et al., 2022) simply divide fMRI signals into $n = 16$ equal parts to obtain sequence features of appropriate length. Zero padding is added if the original length of fMRI signals is not a multiple of 16. We denote such method as 'PatchEmbed'. To evaluate the effectiveness of our design, we conduct experiments by predicting fMRI signals from visual images and generating stimuli images from fMRI signals . As shown in Tab. 5 and Tab. 6, our proposed RoIEmbed achieves better performance than PatchEmbed (34.32 *vs.* 32.88), which clearly demonstrate its efficacy.

For RoIEmbed layer, we extract multi-head features for each RoI region. Here, the number of multi-head is a hyper-parameter. Intuitively, if the number of head is too small (*i.e.*, 1), it may lead to poor representation capacity; On the contrast, a larger number of head may result in information redundancy. To further investigate the affect of this parameter, we report results with different values of heads in the second row of Tab. 5 and Tab. 6 . As expected, it shows a trend of first rising and then falling. The best result is achieved when the number of head is set to 32. Note that we do not tune it for each individual but set it 32 consistently to show the efficacy and generalizability of our proposed layer.

C. MORE QUALITATIVE RESULTS

In this section, we show more visualizations of fMRI decoding (Figs. 7 and 8) and image-fMRI-image reconstruction (Fig. 9).

Table 6: Ablation studies on the effectiveness of RoI-dependent design. Here, we report Pearson correlations between the ground-truth and the predicted fMRI signals of CSI-1 on BOLD5000 dataset.

METHOD	SIZE					
	8	16	24	32	64	96
PatchEmbed (Chen et al., 2022; He et al., 2022)	-	32.88	-	-	-	-
RoIEmbed (*Ours*)	30.72	30.44	31.82	**34.32**	29.67	31.04

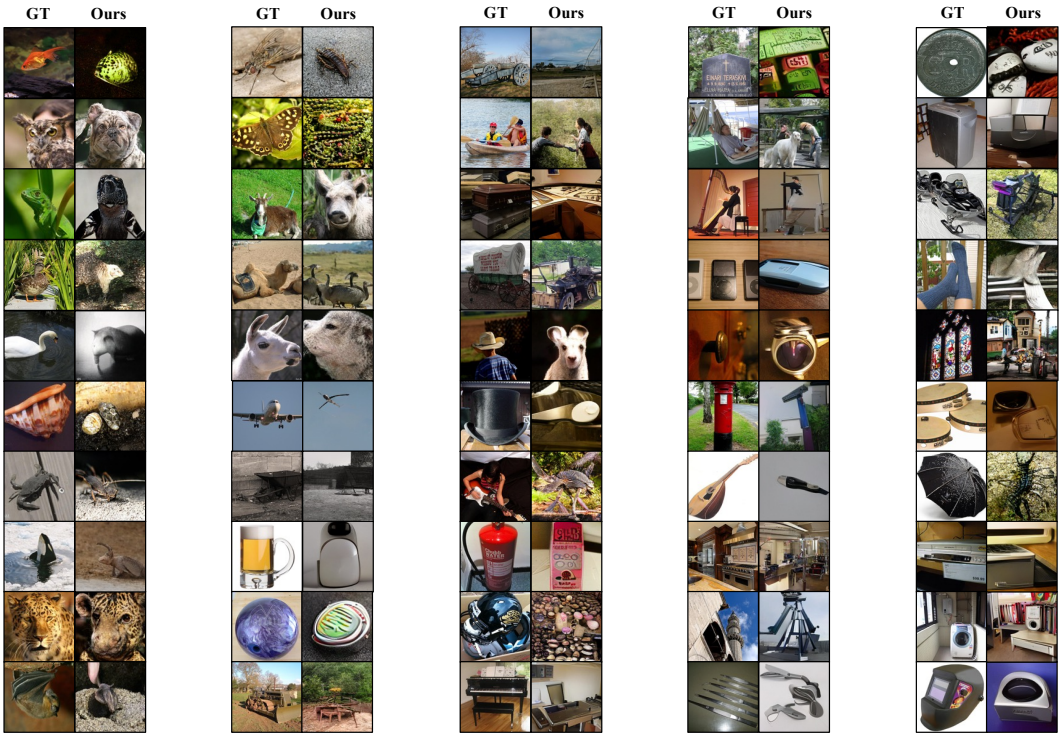

Figure 7: Samples of fMRI decoding on Sbj-3 of the GOD dataset.

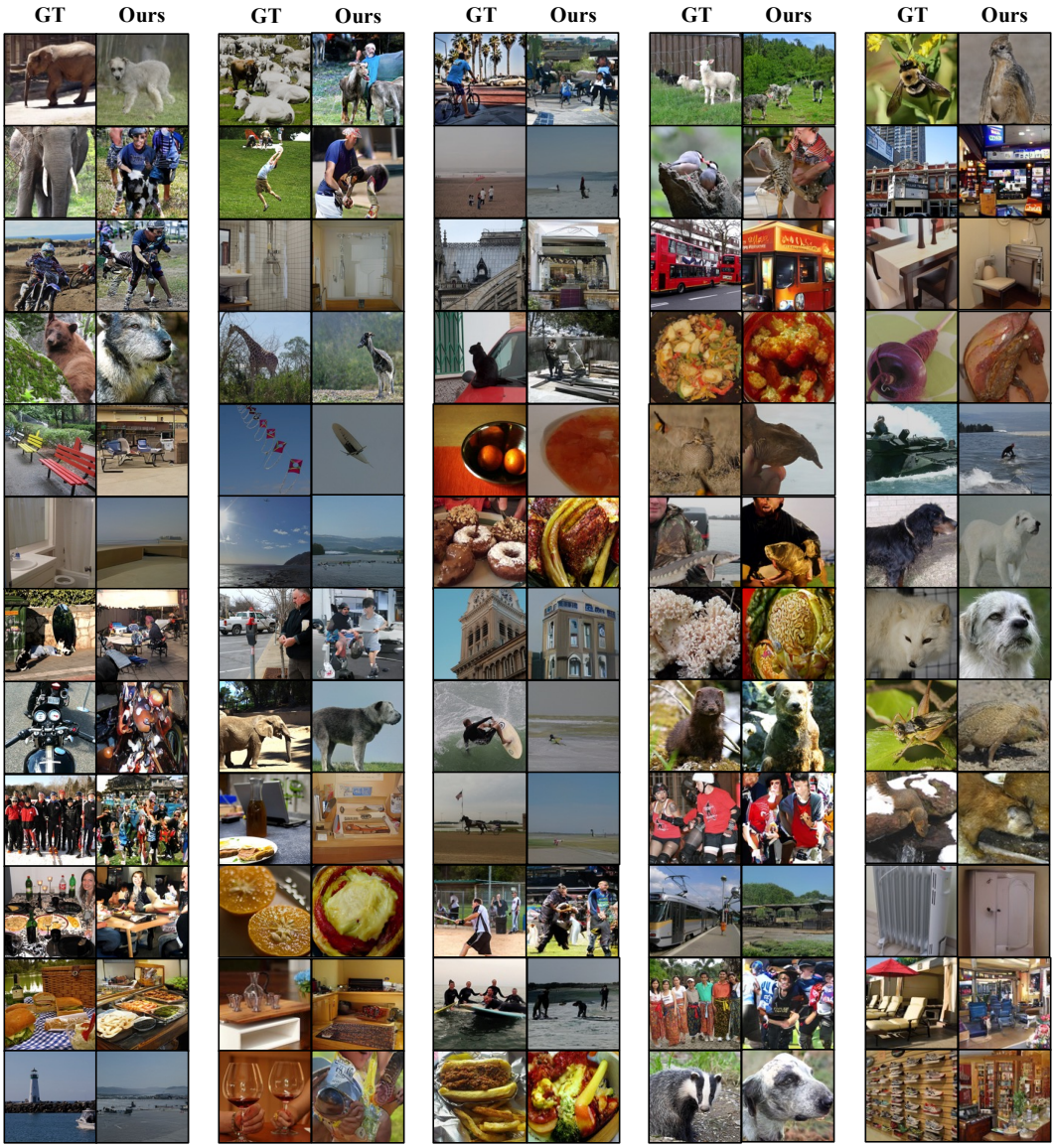

Figure 8: Samples of fMRI decoding on CSI-1 of BOLD5000 dataset.

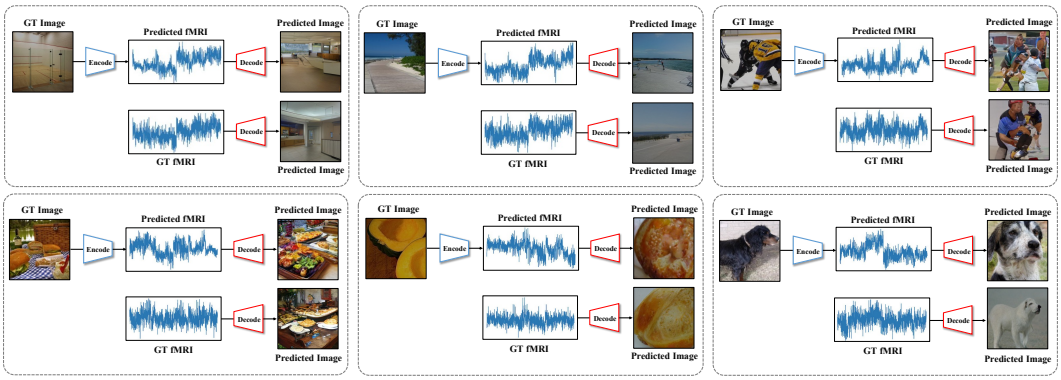

Figure 9: Visualizations of image-fMRI-image reconstruction on CSI-1 of BOLD5000 dataset.

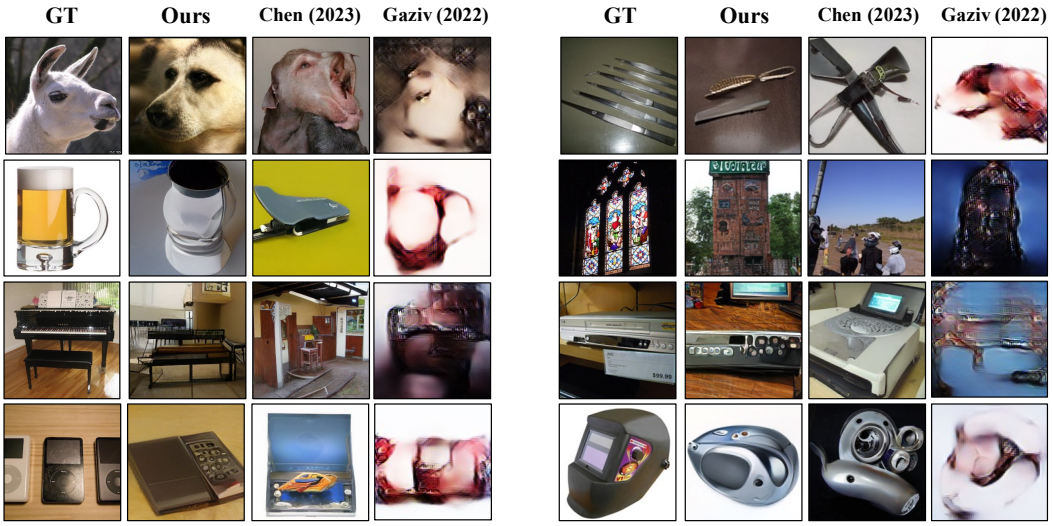

Figure 10: fMRI decoding performance comparison on the GOD dataset.

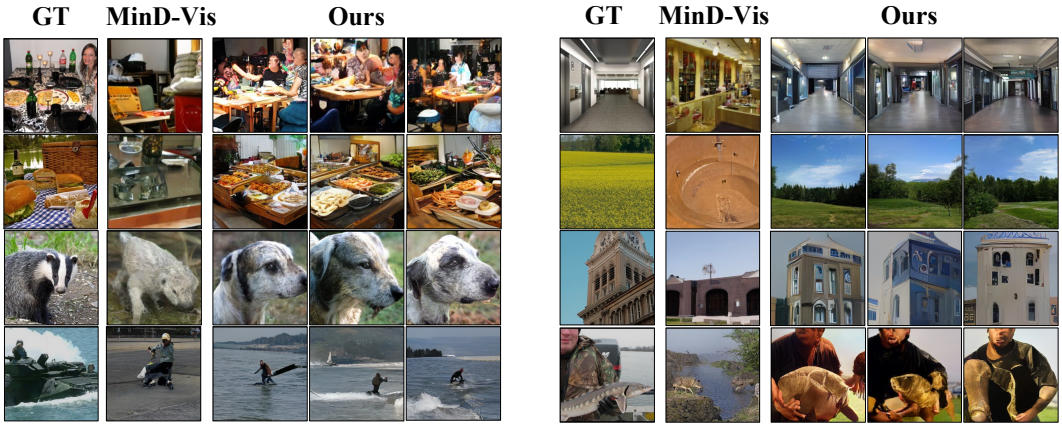

Figure 11: fMRI decoding performance comparison on BOLD5000 dataset.

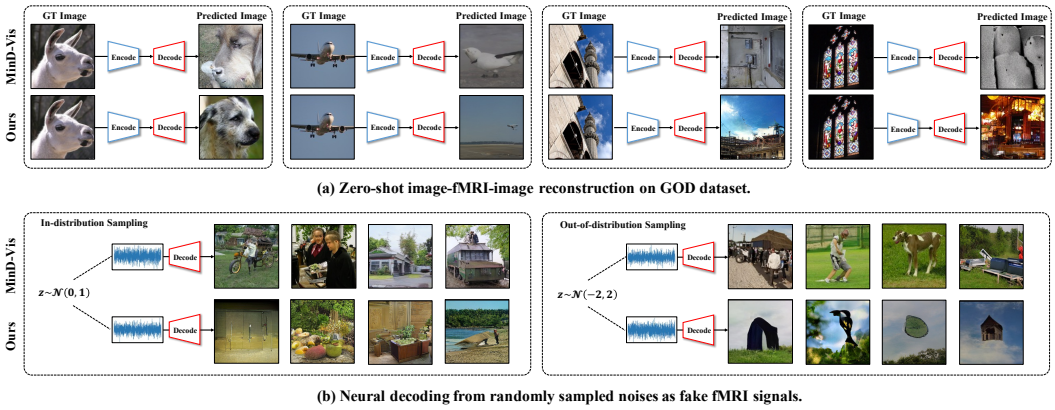

(a) Zero-shot image-fMRI-image reconstruction on GOD dataset.

(b) Neural decoding from randomly sampled noises as fake fMRI signals.

Figure 12: Reliable fMRI decoding analysis.

D. Broader Impact

Our proposed Latent Embedding Alignment (LEA) model provides a unified framework, to efficiently recovers visual stimuli from fMRI signals and predicts brain activity from images. It can serve as a tool to recognize the human perception, read people's mind. We hope it can inspires more valuable and innovative studies in the future, and promote the development of neuroscience. However, the potential negative impact lies in that the usage of this method may cause privacy breach, since people don't want others to pry into their thoughts. Besides, this technology shouldn't be used illegally for any commercial or cognitive strategies. As a result, governments and officials may take action to govern the use of relevant datasets and technologies, and researchers should avoid using datasets that may raise ethical concerns.